Loudspeaker and room response equalization using parallel filters: comparison of pole positioning strategies

Balázs Bank[1]

[1]*Budapest University of Technology and Economics, Dept. of Measurement and Information Systems, H-1521 Budapest, Hungary*

Correspondence should be addressed to Balázs Bank (`bank@mit.bme.hu`)

ABSTRACT
The direct design of fixed-pole parallel second-order filters is a very effective way of obtaining equalizers having the desirable logarithmic frequency resolution for audio applications. The frequency resolution of the parallel filter design is controlled directly by the choice of pole frequencies, similarly to Kautz filters. This paper reviews and compares different pole positioning strategies, such as using a predetermined pole set, warped IIR filter based pole positioning, multi-band warping, and custom warping. In addition, a new technique based on the ripple density of the transfer function is proposed. The methods are tested on loudspeaker and room response equalization applications. It is shown that a predetermined logarithmic pole set gives acceptable equalization despite its simplicity, while the most accurate results for a given filter order are obtained by multi-band and custom warping. The ripple-density based pole positioning presents a useful compromise between accuracy and design complexity.

1. INTRODUCTION

Equalizing the transfer function of loudspeakers and rooms via digital signal processing is subject of research for more than three decades. In its simplest form, only the anechoic response of the loudspeaker is equalized [1, 2, 3, 4], but some of the negative effects of room response can also be compensated [5, 6, 7, 8, 9, 10]. In most cases only the magnitude response of the room is compensated by minimum-phase filtering, thus avoiding the problem coming from inverting non-minimumphase zeros. Some examples include excess-phase compensation as well [9].

It was soon recognized that equalization with a logarithmic frequency resolution is desirable because of two reasons [5, 11]. First, the final judge of quality is the human auditory system, and an equalizer having a resolution similar to the hearing allows a more efficient allocation of computational resources, that is, better quality at the same filter order. Second, due to the wavelength of sound being inversely proportional to its frequency, loudspeaker and room responses measured at different positions in space show more similarity at low frequencies compared to high ones. Therefore, usually a fractional-octave (e.g., third or sixth-octave) smoothing is applied

to the measured magnitude response before inverse filter design.

Another important factor in room and loudspeaker equalization that while peaks of the transfer function should be compensated, the narrow dips should not be inverted. In general, the effects of peaks are strongly audible, while notches are usually unnoticeable. Moreover, dips are strongly position-dependent, and thus the peaks of the equalizer designed to counteract them would actually worsen the response at other points in space [5, 11, 12]. While smoothing itself helps in lessening the problems coming from the inversion of narrow dips of the transfer function, many methods do an explicit dip removal step prior to smoothing [3, 5, 7].

So the first step of loudspeaker and room response equalization is preprocessing the measured response (or, a joint response computed from many measurements) by the removal of dips and applying smoothing. Then the equalizer design is based on this psychoacoustically processed response. The focus of this paper is on the equalizer design, and it is assumed that the measured response(s) are preprocessed with a suitable method.

While the equalizer might be implemented in the fre-

quency domain via fast convolution using FFT, a time-domain implementation is more common due to smaller latency and lower memory need. This is usually realized by FIR [9] or multi-rate FIR filters [5]. Another alternative is the use of special IIR filters with logarithmic-like frequency resolution, such as warped [2], Kautz [13], or parametric second-order filters [3].

It was shown that fixed-pole parallel filters provide a highly efficient way of implementing IIR filters with the desired frequency resolution, resulting in better equalization compared to warped or Kautz filters at a given computational cost [14, 15, 16]. A key point to the accuracy of the parallel filter is the suitable choice of pole frequencies. This paper compares different pole positioning strategies with the application to loudspeaker and room response equalization.

The remainder of the paper is organized as follows. Section 2 reviews the structure of the parallel filter and the algorithm for obtaining the filter weights. This is followed by the overview of the various pole positioning strategies in Sec. 3, based on a loudspeaker–room response equalization example. Then two additional anechoic loudspeaker equalization examples are provided in Sec. 4, and the lessons learned are discussed in Sec. 5. Finally, Sec. 6 concludes the paper.

2. THE PARALLEL FILTER

The general form of the parallel filter consists of a parallel set of second-order sections and an optional FIR filter path [15]:

$$H(z^{-1}) = \sum_{k=1}^{K} \frac{d_{k,0} + d_{k,1}z^{-1}}{1 + a_{k,1}z^{-1} + a_{k,2}z^{-2}} + \sum_{m=0}^{M} b_m z^{-n}, \quad (1)$$

where K is the number of second order sections. The filter structure is depicted in Fig. 1.

2.1. Filter design

Let us first assume that the poles of the parallel filter p_k are known. Then the denominator coefficients are determined by the poles ($a_{k,1} = p_k + \overline{p}_k$ and $a_{k,2} = |p_k|^2$), and the filter design problem becomes linear in its free parameters (weights) $d_{k,0}$, $d_{k,1}$ and b_m.

Using the substitution $z^{-1} = e^{-j\vartheta_n}$ in Eq. (1) and writing it in matrix form for a finite set of ϑ_n angular frequencies yields

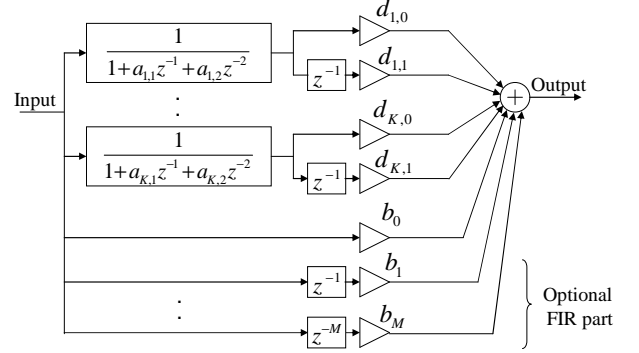$$\mathbf{h} = \mathbf{Mp}, \quad (2)$$

Fig. 1: Structure of the parallel second-order filter.

where $\mathbf{p} = [d_{1,0}, d_{1,1}, \ldots d_{K,0}, d_{K,1}, \ b_0 \ldots b_M]^T$ is a column vector composed of the free parameters. The rows of the modeling matrix $\mathbf{M}$ contain the transfer functions of the second-order sections $1/(1 + a_{k,1}e^{-j\vartheta_n} + a_{k,2}e^{-j2\vartheta_n})$ and their delayed versions $e^{-j\vartheta_n}/(1 + a_{k,1}e^{-j\vartheta_n} + a_{k,2}e^{-j2\vartheta_n})$ for the ϑ_n angular frequencies. The last rows of $\mathbf{M}$ are the transfer functions of the FIR part $e^{-jm\vartheta_n}$ for $m = [0 \ldots M]$. Finally, $\mathbf{h} = [H(\vartheta_1) \ldots H(\vartheta_N)]^T$ is a column vector composed of the resulting frequency response.

Now the task is to find the optimal parameters $\mathbf{p}_{\text{opt}}$ such that $\mathbf{h} = \mathbf{Mp}_{\text{opt}}$ is closest to the target frequency response $\mathbf{h}_{\text{t}} = [H(\vartheta_1)_{\text{t}} \ldots H(\vartheta_N)_{\text{t}}]^T$. If the error is evaluated in the mean squares sense

$$e_{\text{LS}} = \sum_{n=1}^{N} |H(\vartheta_n) - H(\vartheta_n)_{\text{t}}|^2 = (\mathbf{h} - \mathbf{h}_{\text{t}})^H (\mathbf{h} - \mathbf{h}_{\text{t}}), \quad (3)$$

the minimum of Eq. (3) is found by the well-known least-squares (LS) solution

$$\mathbf{p}_{\text{opt}} = (\mathbf{M}^H \mathbf{M})^{-1} \mathbf{M}^H \mathbf{h}_{\text{t}}, \quad (4)$$

where $\mathbf{M}^H$ is the conjugate transpose of $\mathbf{M}$.

Note that Eq. (4) assumes a filter specification $H_{\text{t}}(\vartheta_n)$ given for the full frequency range $\vartheta_n \in [-\pi, \pi]$. In most of the cases we are interested in filters with real coefficients: in this case either the user has to ensure that $H_{\text{t}}(-\vartheta_n) = \overline{H}_{\text{t}}(\vartheta_n)$, where $\overline{H}_{\text{t}}$ is the complex conjugate of H_{t}, or, in the case of one sided ($\vartheta_n \in [0, \pi]$) specifications, the following formula has to be used instead of Eq. (4):

$$\mathbf{p}_{\text{opt}} = (\text{Re}\left\{\mathbf{M}^H \mathbf{M}\right\})^{-1} \text{Re}\left\{\mathbf{M}^H \mathbf{h}_{\text{t}}\right\}, \quad (5)$$

where $\text{Re}\{\mathbf{A}\}$ corresponds to taking the real part of $\mathbf{A}$.

2.2. Direct equalizer design

Equalizing a system by the parallel filter can be done by dividing the desired target response $H_t(\vartheta_n)$ by the system response $H_s(\vartheta_n)$ and designing a parallel filter for this $H_t(\vartheta_n)/H_s(\vartheta_n)$ specification according to Sec. 2.1. However, the mathematically correct way of designing an equalizer is to minimize the error between the final, equalized response $H_{eqd}(\vartheta_n)$ and the target frequency response $H_t(\vartheta_n)$ [15]. This is basically a system identification problem with output error minimization: the input of the parallel filter is the system response $H_s(\vartheta_n)$ and we should estimate the filter parameters such that its output $H_{eqd}(\vartheta_n)$ best matches the target response $H_t(\vartheta_n)$.

Accordingly, the equalized response is given by

$$H_{eqd}(z^{-1}) = H(z^{-1})H_s(z^{-1}) =$$
$$\sum_{k=1}^{K} \frac{d_{k,0} + d_{k,1}z^{-1}}{1 + a_{k,1}z^{-1} + a_{k,2}z^{-2}} H_s(z^{-1}) + \sum_{m=0}^{M} b_m z^{-n} H_s(z^{-1}). \tag{6}$$

Writing this in a matrix form for a finite set of ϑ_n angular frequencies yields

$$\mathbf{h}_{eqd} = \mathbf{M}_{eq}\mathbf{p}_{eq}, \tag{7}$$

where $\mathbf{p}_{eq} = [d_{1,0}, d_{1,1}, \dots d_{K,0}, d_{K,1}, b_0 \dots b_M]^T$ is a column vector composed of the free parameters of the parallel equalizer. The equalizer modeling matrix $\mathbf{M}_{eq}$ is obtained from the modeling matrix $\mathbf{M}$ of Sec. 2.1 by multiplying all rows of $\mathbf{M}$ by the system frequency response $H_s(\vartheta_n)$. Finally, $\mathbf{h}_{eqd} = [H_{eqd}(\vartheta_1) \dots H_{eqd}(\vartheta_N)]^T$ is a column vector composed of the resulting final frequency response. Since Eq. (7) has the same structure as Eq. (2), the optimal set of parameters are obtained in the same way as in Sec. 2.1 by Eqs. (4) or (5).

3. POLE POSITIONING COMPARISON

A loudspeaker-room response equalization example will be used for comparing the different pole positioning approaches. The original (unsmoothed) response is displayed in Fig. 2 (a), together with its one-octave smoothed version with dashed line. The one-octave smoothed version is used for limiting the dips in the transfer function: everything below 6dB of this smoothed
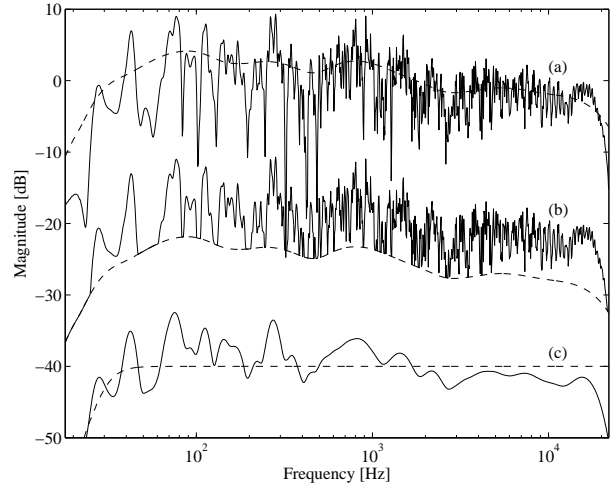

Fig. 2: The loudspeaker–room response used in the comparison: (a) the measured response together with its one-octave smoothed version with dashed line, (b) the measured response limited by the smoothed response decreased by 6dB (limit shown by dashed line), and (c) the limited response smoothed at sixth- and third-octave resolution below and above 500 Hz, respectively.

response is substituted by the smoothed response itself. This is shown in Fig. 2 (b), where the limit is displayed by dashed line, and a limited transfer function by solid line. Finally, this limited response is smoothed with a sixth-octave resolution below 500 Hz and a third-octave resolution above, shown in Fig. 2 (c). The target response is displayed in Fig. 2 (c) dashed line. The target is chosen to be a simple high-pass filter for easier visualization of the equalization results. Note that in practice this does not lead to optimal sound, and typically we would desire a target with a downward slope [7]. Also, more sophisticated methods are available for removing the sharp dips of the response, which can take into account multiple measurements, see, e.g., [7]. As this paper focuses on the filter design problem, it is sufficient to have a processed room response that is similar in structure to what would have been obtained by the state-of-the-art room response correction methods.

In all cases the equalizers are designed by the direct equalizer design method of Sec. 2.2, and the only difference is in how the pole positions are obtained.

3.1. Pole positioning with a predetermined

pole set

The simplest way of choosing the poles is setting them according to the required resolution. For obtaining a $1/\beta$ octave resolution, $\beta/2$ poles are inserted in each octave [17]. Then, the poles of the parallel filter, p_k, are computed using the following formulas [17]:

$$\theta_k = \frac{2\pi f_k}{f_s} \tag{8a}$$

$$p_k = e^{-\frac{\Delta\theta_k}{2}}e^{\pm j\theta_k}, \tag{8b}$$

where θ_k are the pole frequencies in radians given by the predetermined analog frequency series f_k and the sampling frequency f_s. The bandwidth of the kth second-order section $\Delta\theta_k$ is computed from the neighboring pole frequencies

$$
\begin{aligned}
\Delta\theta_k &= \tfrac{\theta_{k+1}-\theta_{k-1}}{2} &\quad \text{for } k=[2,..,K-1] \\
\Delta\theta_1 &= \theta_2 - \theta_1 \\
\Delta\theta_K &= \theta_K - \theta_{K-1}.
\end{aligned} \tag{9}
$$

Equation (8b) sets the pole radii $|p_k|$ in such a way that the transfer functions of the parallel sections cross approximately at their -3dB points.

Since the target has sixth-octave resolution below 500 Hz, we place 3 poles per octave in the low frequency region, while 1.5 poles per octave above, where the target was smoothed to third-octave. This leads to a total number of 20 pole pairs, that is, 20 second-order sections (the filter order is 40).

The result of the equalization is displayed in Fig. 3 (b), showing an acceptable performance since the ripples of the equalized transfer function are within ± 1 dB around the target response. Note that now the parallel filter was designed using the smoothed response for making the comparison with other pole positioning approaches easier. However, the greatest advantage of using a predetermined pole set besides its simplicity is that it does not require the smoothing of the measured transfer function. This is because the parallel filter design performs smoothing "automatically" based on its pole density, as was demonstrated in [17].[1]

---

[1]For all the other pole positioning strategies this is not the case. While the weights of the parallel filter could be estimated from the unsmoothed response directly in all cases, the following pole positioning methods all require a smoothed response to work properly. And once we had to smooth the response anyway, it is practical to estimate the
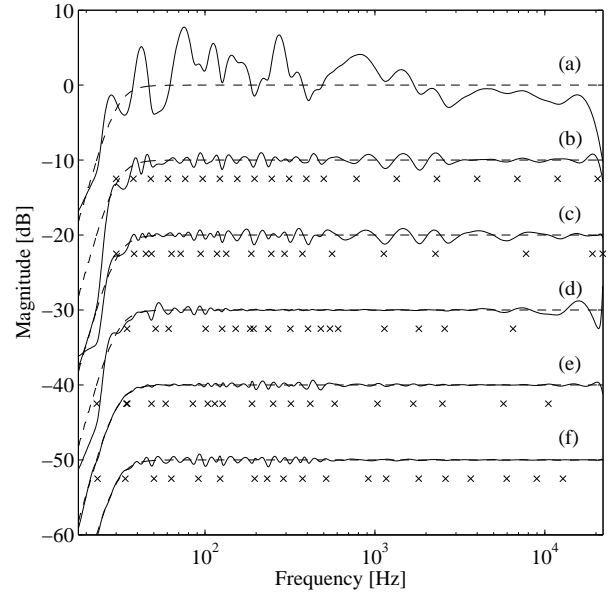

Fig. 3: Comparison of different pole positioning techniques for loudspeaker–room response equalization. The processed room response is displayed in (a). The pole positioning techniques used are (b) predetermined pole set, pole positioning based on (c) ripple density, (d) standard warped IIR filter design, (e) multi-band warping, and (f) custom warping. The target response is shown by dashed lines. The pole frequencies are displayed by crosses. The number of pole-pairs (or, second-order sections) is 20 in all cases, giving a total filter order 40.

3.2. Ripple-density based pole positioning

A drawback of using a predetermined pole set is that the user has to choose how many poles he/she would like to use in a certain region of the transfer function. Here a new method is proposed which chooses the pole frequencies based on the processed system response, without any prior knowledge on the type of smoothing applied.

The basic idea of the method is that in those regions where there are more ripples in the transfer function, more poles are needed. The steps of the algorithm are explained using Fig. 4. The smoothed transfer function

---

weights from the smoothed response instead of the original one. The benefit of doing so is that smaller number of specification points are sufficient, thus, the computational complexity of the LS weight estimation is decreased.

is shown in Fig. 4 (a). The first step of the algorithm is computing the absolute difference of the adjacent frequency response points in dB scale. The level of this function will be proportional to the raggedness of the transfer function, so it is called ripple density. It is displayed in Fig. 4 (b). The goal is now to divide this ripple density function in as many equal areas as many poles we would like to use, and the borders of these areas will be chosen as pole frequencies. This is in practice done by integrating (in practice cumulating) the density function giving the ripple distribution function. Then this is scaled so that it goes from zero to the number of pole frequencies minus one, displayed in Fig. 4 (c). Finally, whenever this distribution function is integer (crosses a horizontal line in Fig. 4 (c)) a pole frequency is obtained, displayed by crosses. The same pole frequencies are also displayed in Fig. 4 (a), showing that indeed more poles are placed in those regions where the response is more ragged. Note that this simple procedure gives the pole frequencies only: the pole radii (or Q factors) are determined by Eqs. (8) and (9) as before, and not based on the actual Q factors of the resonances of the system.

The equalization using a ripple-density based pole set is shown in Fig. 3 (c), leading to a similar performance to the predetermined pole set in this case.

3.3. Pole positioning based on a standard warped IIR design

Compared to the simple techniques presented above, better equalization can be achieved if the pole positions are obtained using an IIR filter design. Since we are designing filters with a logarithmic resolution, the use of frequency warping [18, 19] is mandatory. The most straightforward way is to design a single warped IIR filter using the smoothed response, find the poles and dewarp them [20].

In the example of Fig. 3 (d), a 40th order IIR filter is identified by the frequency-domain Steiglitz-McBride method [21] based on the warped version of the smoothed response as the input and the warped version of the target as the output. The frequency axis is transformed by

$$\tilde{\vartheta} = \nu(\vartheta) = \arctan \frac{(1 - \lambda^2)\sin(\vartheta)}{(1 + \lambda^2)\cos(\vartheta) - 2\lambda}, \qquad (10)$$

where ϑ is the original and $\tilde{\vartheta}$ is the warped angular frequency in radians [19]. In our example, a warping parameter $\lambda = 0.95$ is used, and the responses are made
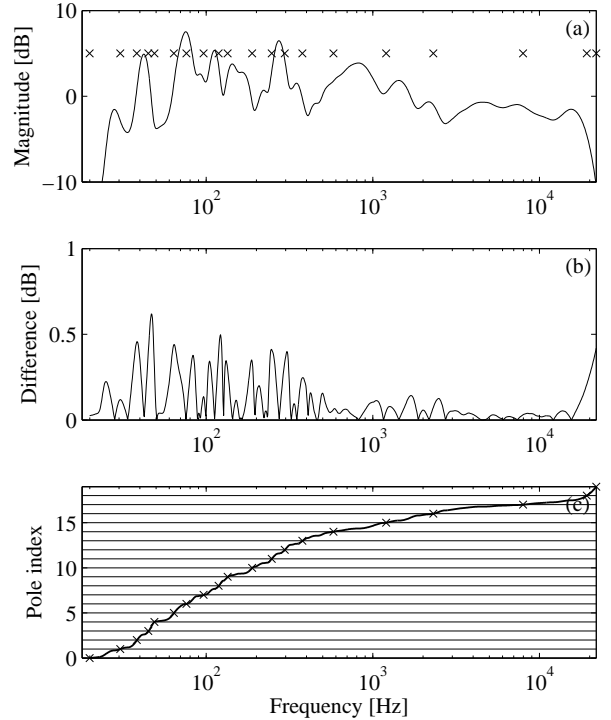

Fig. 4: Steps of ripple-density based pole positioning: (a) the smoothed system response, (b) the ripple density (the difference between the adjacent points of the smoothed response), and (c) the ripple distribution (scaled cumulative sum of ripple density). In (c) horizontal lines show the pole indices. The pole frequencies are displayed by crosses in (a) and (c).

minimum-phase prior to using the frequency-domain Steiglitz-McBride algorithm [21]. Then, the poles $\tilde{p}_k$ of the identified IIR filter are obtained, and dewarped by the following expression [19]:

$$p_k = \frac{\tilde{p}_k + \lambda}{1 + \lambda \tilde{p}_k}. \qquad (11)$$

It can be seen in Fig. 3 (d) that the warping based pole positioning provides more accurate equalization compared to the first two methods, and its only shortcoming that the accuracy is concentrated in the middle frequency range. By increasing λ, it is possible to decrease the the low-frequency errors, at the price of increasing the high-frequency ones, but there is actually no such λ value which would lead to an even distribution of the fre-

quency resolution on the logarithmic scale. This problem is addressed by multi-band warping.

3.4. Pole positioning based on multi-band warping

In multi-band warping the transfer function is divided into separate frequency bands, and different warping parameters are used in each band so that the warping effect is maximized in each region. Then, separate warped IIR filters are designed for the different regions, their poles are dewarped, and finally the pole sets are united [16].

In the example of Fig. 3 (e), dual-band warping is applied. The split frequency is 500 Hz, which is the same frequency where the smoothing resolution changes from sixth- to third-octave. The out-of-band parts of the responses are made flat prior to filter design to assure that the IIR designs produce poles only in their respective frequency bands [16]. For the low-frequency region $\lambda_{\mathrm{LF}} = 0.986$ is used, while for the high-frequency region, the warping parameter is set to $\lambda_{\mathrm{HF}} = 0.65$. These values maximize the warping effect in the middle of their bands [16], but of course it is possible to adjust them for tailoring the performance of the filters. The filter orders are 26 and 14 in the low and high bands, respectively. Once the two warped IIR filters are designed in a similar way as discussed in Sec. 3.3, their poles are dewarped using the corresponding λ_{LF} and λ_{HF} values in Eq. (11) and the two pole sets are united, giving a total filter order of 40.

Figure 3 (e) shows that the frequency resolution is now spread much more evenly on the logarithmic scale and thus an excellent equalization performance is achieved for the same filter order as in the previous methods. The only ripples that can be seen are in the transition region of the two bands, but their amplitude is ± 0.5 dB around the target, so they can be considered negligible. The price to pay compared to the simple warping of Sec. 3.3 is the additional complexity of separating the response to different regions and the need of designing multiple filters. However, the total order of filters remains the same, so the design complexity is not increased significantly. A small shortcoming is that the user has to balance between the number of poles used in the two frequency bands.

3.5. Pole positioning based on custom warping

Unlike in traditional warping, where the frequency mapping is determined by a single parameter λ according to Eq. (10), in custom warping arbitrary mappings $\tilde{\vartheta} = \nu(\vartheta)$ can be used [22]. As the goal is to obtain logarithmic frequency resolution, it is logical to use a logarithmic mapping. Here we use the warping function proposed in [23] which is linear below a frequency limit ϑ_c and logarithmic above. The linear function is chosen so that the derivative does not jump at ϑ_c:

$$\tilde{\vartheta} = \nu(\vartheta) = \begin{cases} a\vartheta & \text{if } 0 \leq \vartheta < \vartheta_{\mathrm{c}} \\ \pi \frac{\ln(b\vartheta)}{\ln(b\pi)} & \text{if } \vartheta_{\mathrm{c}} \leq \vartheta < \pi \end{cases} \quad (12a)$$

$$a = \frac{\pi}{\vartheta_{\mathrm{c}}(1 + \ln(\pi/\vartheta_c))}, \quad (12b)$$

$$b = \frac{e}{\vartheta_{\mathrm{c}}}, \quad (12c)$$

where $e = e^1 = \exp(1)$. Let us also define the inverse mapping $\nu^{-1}(\tilde{\vartheta})$ so that $\vartheta = \nu^{-1}(\nu(\vartheta))$.

Once the smoothed system response and the target response are warped according to the frequency transform of Eq. (12), an IIR filter is identified again using the frequency-domain Steiglitz-McBride algorithm [21], and its poles $\tilde{p}_k$ are found.

However, becuase of the nonstandard warping profile, the poles cannot be dewarped with Eq. (11). For complex poles, we first compute the pole frequencies $\tilde{\vartheta}_{p,k} = \varphi\{\tilde{p}_k\}$ and radii $\tilde{r}_{p,k} = |\tilde{p}_k|$. Then, the dewarped poles p_k arise as

$$\vartheta_{p,k} = \nu^{-1}(\tilde{\vartheta}_{p,k}), \quad (13a)$$

$$r_{p,k} = \tilde{r}_{p,k}^{\nu^{-1\prime}(\tilde{\vartheta}_{p,k})}, \quad (13b)$$

$$p_k = r_{p,k} e^{j\vartheta_{p,k}}, \quad (13c)$$

that is, the pole frequencies are mapped according to the inverse mapping function $\nu^{-1}(\tilde{\vartheta})$ and the radii are raised to the power according to the derivative of the inverse mapping function $\nu^{-1\prime}(\tilde{\vartheta})$. For real poles we compute their frequencies (the -3dB point of their transfer functions) and remap them by $\nu^{-1}(\tilde{\vartheta})$ [22].

The equalization using poles obtained by custom warping is displayed in Fig. 3 (f). The performance is very similar to the multi-band warping case, only that the ripply region is now at lower frequencies. The ripples are still within ± 0.5 dB around the target, so they can be considered inaudible. The computational complexity of the design is similar to the other two warped designs. A benefit compared to the multi-band warping is that only
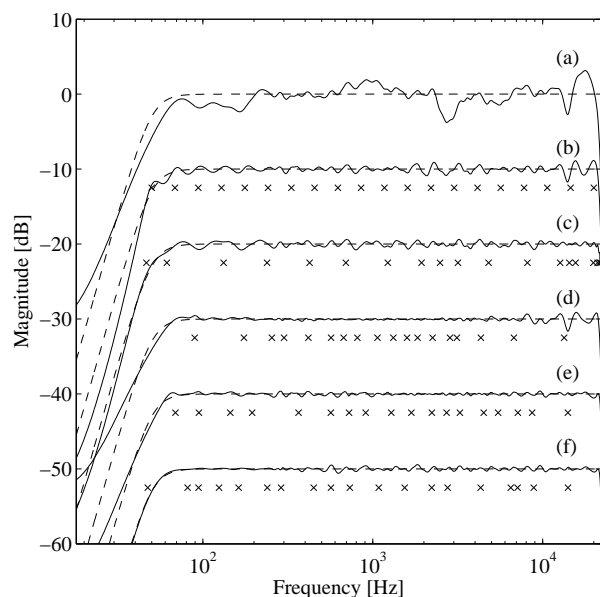
Fig. 5: Comparison of different pole positioning techniques for a floorstanding loudspeaker response equalization. The 12th-octave smoothed anechoic loudspeaker response is displayed in (a). The pole positioning techniques used are (b) predetermined pole set, pole positioning based on (c) ripple density, (d) standard warped IIR filter design, (e) multi-band warping, and (f) custom warping. The target response is shown by dashed lines. The pole frequencies are displayed by crosses. The number of pole-pairs (or, second-order sections) is 20 in all cases, giving a total filter order 40.

the total filter order has to be given by the user, and not the orders in the different bands as in Sec. 3.4.

4. ADDITIONAL EXAMPLES

Here additional equalization examples are presented to give a broader view on the behavior of the different methods. First the anechoic response of the same two-way floorstanding loudspeaker is equalized which was used in a room in the previous example. Now the measured anechoic frequency response is smoothed at 12th-octave resolution and no dip removal is applied. This is shown in Fig. 5 (a).

For the predetermined pole set, while 12th-octave resolution would require higher pole density to perfectly equal-

ize the response (six pole pairs per octave actually leads to 51 pole pairs), we use 20 pole pairs between 50 Hz and 20 kHz, since for the more sophisticated methods this filter order is sufficient to obtain practically perfect equalization, as we shall see later. The results are acceptable, the ripples are within ± 1 dB, as can be seen in Fig. 5 (b). Since now there are some regions which are more ragged than others, the ripple-density based pole positioning leads to slightly improved results, because it is able to concentrate the frequency resolution to more problematic regions (see Fig. 5 (c)).

For this example $\lambda = 0.85$ gives the best results for warping-based pole positioning, shown in Fig. 5 (d). Similarly to Fig. 3 (d), the accuracy is concentrated to the middle range, while the band edges are less accurately equalized. This is again overcome by the multi-band (Fig. 5 (e)) and custom warping (Fig. 5 (f)).

The next example is a two-way bookshelf speaker having some distinct spikes in its frequency response. The response is smoothed with a 12th-octave resolution prior to equalizer design, displayed in Fig. 6 (a).

First, a predetermined pole set is used with 20 pole pairs logarithmically distributed between 70 Hz and 20 kHz. The equalizer has a poor performance as seen in Fig. 5 (b), because the pole density is too low in the problematic regions. On the other hand, the ripple-density based pole positioning can show its power: equalization improves significantly, since now the poles are concentrated in the ragged parts of the frequency response (see Fig. 5 (c)).

In this case $\lambda = 0.8$ is used for warping-based pole positioning in Fig. 5 (d). On the contrary to the previous examples, even simple warping can provide perfect equalization. This is because the design bandwidth is smaller, thus, we do not face with the problems we had in the band edges for Fig. 3 (d) and Fig. 5 (d). Thus, the multi-band (Fig. 6 (e)) and custom warping (Fig. 6 (f)) do not provide any additional benefit in this case. Actually, their performance is less preferable.

5. DISCUSSION

Now that we have reviewed the different pole positioning strategies for parallel filter design and have seen a couple of examples, some conclusions can be drawn about the benefits of the various methods.

Predetermined pole set: This is the simplest method, which works relatively well for loudspeaker–room responses, since room responses have so many resonances
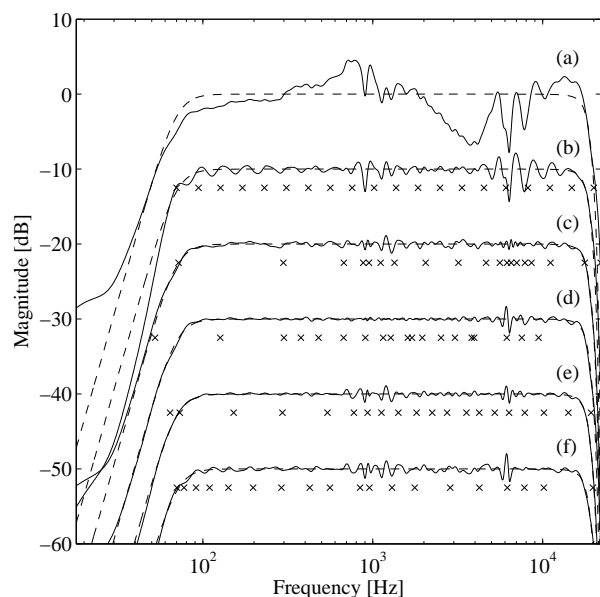
Fig. 6: Comparison of different pole positioning techniques for a bookshelf loudspeaker response equalization. The 12th-octave smoothed anechoic loudspeaker response is displayed in (a). The pole positioning techniques used are (b) predetermined pole set, pole positioning based on (c) ripple density, (d) standard warped IIR filter design, (e) multi-band warping, and (f) custom warping. The target response is shown by dashed lines. The pole frequencies are displayed by crosses. The number of pole-pairs (or, second-order sections) is 20 in all cases, giving a total filter order 40.

that the ripplyness of smoothed response is determined by the smoothing itself. However, when the raggedness is unevenly distributed in the response, such as in Fig. 6, a logarithmic pole positioning is not adequate, and regions with different pole density should be selected manually, which is not practical. The main advantage of the method is that there is actually no need for transfer function smoothing prior to equalizer design, so the equalizer can be obtained from the measured response directly.

Ripple-density based pole positioning: This method, while simple enough, works robustly in all cases since it allocates the frequency resolution in accordance with the raggedness of the response. It shows its main benefits compared to the predetermined pole set when the response has some specific problematic regions.

Warping based pole positioning: Since this method is based on a warped IIR filter design, it is able to actually take into account both the frequencies and Q factors of the peaks and valleys of the response. When the system is not using the full audio bandwidth (such as in small bookshelf or multimedia speakers) it provides perfect equalization. Systems having full audio bandwidth will suffer from low- and high-frequency inaccuracies when using this pole positioning method. We also note here that the response of the parallel filter using a warping based pole set is practically the same as what would have been obtained using a warped IIR filter of the same order.

Pole positioning using multi-band warping: This method overcomes the bandwidth limitation of straightforward warping, thus, it can be safely used for any type of frequency responses with excellent results. The only slight shortcoming is that the user has to adjust the crossover frequency and the filter orders of the frequency bands.

Pole positioning using custom warping: This method provides a similar performance compared to multi-band warping. A slight benefit is that only the total filter order has to be given by the user and no additional interaction is necessary.

6. CONCLUSION

This paper has compared various pole positioning strategies used for fixed-pole parallel filter design with the application to loudspeaker and room response equalization. The simplest of all techniques is using a predetermined pole set, where the pole frequencies are set according to a predetermined (typically logarithmic) distribution. This gives generally acceptable results when the raggedness of the response is distributed relatively evenly as a function of frequency, which is the case for smoothed room responses, and also for well behaving loudspeaker responses.

A new method, the ripple-density based pole positioning was proposed which automatically determines the pole density based on the raggedness of the response. This is a useful alternative to the predetermined pole set, because while it is still simple, it is more robust against uneven distribution of the resonances in the response, and requires no interaction from the user.

The best equalization is obtained with a pole set determined by the methods based on warped IIR filter designs.

For systems having smaller bandwidth (such as small multimedia loudspeakers), straightforward warped IIR design gives excellent results, while for systems having wider bandwidth, multi-band or custom warping should be used.

While in this paper only equalization examples were presented, the conclusions drawn are perfectly valid for loudspeaker and room response modeling, and to a major extent also for modeling and equalization of other systems.

MATLAB code for designing fixed-pole parallel filters can be downloaded from
`http://www.mit.bme.hu/~bank/parfilt`

7. ACKNOWLEDGEMENT

8. REFERENCES

[1] J. N. Mourjopoulos, P. M. Clarkson, and J. K. Hammond. A comparative study of least-squares and homomorphic techniques for the inversion of mixed phase signals. In *Proc. IEEE Int. Conf. Acoust. Speech and Signal Process.*, pages 1858–1861, May 1982.

[2] Matti Karjalainen, Esa Piirilä, Antti Järvinen, and Jyri Huopaniemi. Comparison of loudspeaker equalization methods based on DSP techniques. *J. Audio Eng. Soc.*, 47(1–2):14–31, Jan./Feb. 1999.

[3] Germán Ramos and José J. López. Filter design method for loudspeaker equalization based on IIR parametric filters. *J. Audio Eng. Soc.*, 54(12):1162–1178, Dec. 2006.

[4] Germán Ramos, José J. López, and Basilio Pueo. Combination of warped and linear filter structures for loudspeaker equalization. In *Proc. 124th AES Conv., Preprint No. 7401*, Amsterdam, The Netherlands, 2008.

[5] Peter G. Craven and Michael A. Gerzon. Practical adaptive room and loudspeaker equalizer for hi-fi use. In *Proc. 92nd AES Conv., Preprint No. 3346*, Vienna, Austria, Mar. 1992.

[6] Aki Mäkivirta, Poju Antsalo, Matti Karjalainen, and Vesa Välimäki. Modal equalization of louspeaker-room responses at low frequencies. *J. Audio Eng. Soc.*, 51(5):324–343, May 2003.

[7] Jan Abildgaard Pedersen and Kasper Thomsen. Fully automatic loudspeaker–room adaptation – The RoomPerfect system. In *Proc. AES 32nd Int. Conf. "DSP for Loudspeakers"*, pages 11–20, Hillerød, Denmark, Sep. 2007.

[8] Jakob Dyreby and Sylvian Choisel. Equalization of loudspeaker resonances using second-order filters based on spatially distributed impulse responses. In *Proc. 123rd AES Conv., Preprint No. 7205*, New York, USA, Feb. 2007.

[9] L.-J. Brännmark and A. Ahlén. Spatially robust audio compensation based on SIMO feedforward control. *IEEE Trans. Signal Process.*, 57(5):1689–1702, May 2009.

[10] A. Carini, S. Cecchi, F. Piazza, Ivan Omiciuolo, and G. L. Sicuranza. Multiple position room equalization in the frequency domain. *IEEE Trans. Audio, Speech, and Lang. Process.*, 20(1):122–135, Jan. 2012.

[11] Matti Karjalainen, Tuomoas Paatero, John N. Mourjopoulos, and Panagiotis D. Hatziantoniou. About room response equalization and dereverberation. In *Proc. IEEE Workshop Appl. of Signal Process. to Audio and Acoust.*, pages 183–186, New Paltz, NY, USA, Oct. 2005.

[12] Floyd E. Toole. Loudspeakers and rooms for sound reproduction–A scientific review. *J. Audio Eng. Soc.*, 54(6):451–476, June 2006.

[13] Matti Karjalainen and Tuomas Paatero. Equalization of loudspeaker and room responses using Kautz filters: Direct least squares design. *EURASIP J. on Advances in Sign. Proc., Spec. Iss. on Spatial Sound and Virtual Acoustics*, 2007:13, 2007. Article ID 60949, doi:10.1155/2007/60949.

[14] Balázs Bank. Perceptually motivated audio equalization using fixed-pole parallel second-order filters. *IEEE Signal Process. Lett.*, 15:477–480, 2008. URL: `http://www.acoustics.hut.fi/go/spl08-parfilt`.

[15] Balázs Bank. Logarithmic frequency scale parallel filter design with complex and magnitude-only specifications. *IEEE Signal Process. Lett.*, 18(2):138–141, Feb. 2011.

[16] Balázs Bank and Germán Ramos. Improved pole positioning for parallel filters based on spectral smoothing and multi-band warping. *IEEE Signal Process. Lett.*, 18(5):299–302, Mar. 2011.

[17] Balázs Bank. Audio equalization with fixed-pole parallel filters: An efficient alternative to complex smoothing. In *Proc. 128th AES Conv., Preprint No. 7965*, London, UK, May 2010.

[18] Michael Waters and Mark B. Sandler. Least squares IIR filter design on a logarithmic frequency scale. In *Proc. IEEE Int. Symp. on Circuits and Syst.*, pages 635–638, May 1993.

[19] Aki Härmä, Matti Karjalainen, Lauri Savioja, Vesa Välimäki, Unto K. Laine, and Jyri Huopaniemi. Frequency-warped signal processing for audio applications. *J. Audio Eng. Soc.*, 48(11):1011–1031, Nov. 2000.

[20] Balázs Bank. Direct design of parallel second-order filters for instrument body modeling. In *Proc. Int. Computer Music Conf.*, pages 458–465, Copenhagen, Denmark, Aug. 2007. URL: `http://www.acoustics.hut.fi/go/icmc07-parfilt`.

[21] Leland B. Jackson. Frequency-domain Steiglitz-McBride method for least-squares filter design, ARMA modeling, and periodogram smoothing. *IEEE Signal Process. Lett.*, 15:49–52, 2008.

[22] Balázs Bank. Warped IIR filter design with custom warping profiles and its application to room equalization. In *Proc. 130th AES Conv., Preprint No. 7965*, London, UK, May 2011.

[23] Aki Härmä and Tuomas Paatero. Discrete representation of signals on a logarithmic frequency scale. In *Proc. IEEE Workshop Appl. of Signal Process. to Audio and Acoust.*, New Paltz, NY, USA, Oct. 2001.